Combination therapy with EGFR tyrosine kinase inhibitors and TEAD inhibitor increases tumor suppression effects in *EGFR* mutation-positive lung cancer

Authors and affiliations

Tatsuya Ogimoto[1], Hiroaki Ozasa[1], Takahiro Tsuji[1,2], Tomoko Funazo[1], Masatoshi Yamazoe[1], Kentaro Hashimoto[1], Hiroshi Yoshida[1], Kazutaka Hosoya[1], Hitomi Ajimizu[1], Takashi Nomizo[1], Hironori Yoshida[1], Masatsugu Hamaji[3], Toshi Menju[3], Akihiko Yoshizawa[4], Hiroshi Date[3], Toyohiro Hirai[1]

[1] Department of Respiratory Medicine, Graduate School of Medicine, Kyoto University, Kyoto, Japan

[2] Department of Anatomy and Molecular Cell Biology, Graduate School of Medicine, Nagoya University, Nagoya, Japan

[3] Department of Thoracic Surgery, Graduate School of Medicine, Kyoto University, Kyoto, Japan

[4] Department of Diagnostic Pathology, Kyoto University Hospital, Kyoto, Japan

Running title

TEAD inhibitor is effective in *EGFR*-mutated lung cancer

Keywords

Lung cancer, EGFR, EGFR-TKI, YAP1, TEAD inhibitor

Corresponding author

Hiroaki Ozasa, M.D., Ph.D.

Department of Respiratory Medicine, Graduate School of Medicine, Kyoto University,

54 Shogoin-kawahara-cho, Sakyo-ku, Kyoto 606-8507, Japan.

Phone: +81 75 751 3830. Fax: +81 75 751 4643.

E-mail address: ozahiro@kuhp.kyoto-u.ac.jp

Financial support

This study was supported by JST SPRING, grant number JPMJSP2110 (T.O.), and JSPS KAKENHI, grant number 19K08601 (H.O.).

Conflicts of interest

H. Ozasa received VT103 and VT104 from Vivace Therapeutics Inc. H. Yoshida received

honoraria for speaker's bureaus from Chugai Pharmaceutical Co. Ltd. and AstraZeneca K.K. The other authors declare no conflicts of interest.

Word count: 3997

Number of figures: 6

Number of tables: 0

Number of supplementary figures: 11

Number of supplementary tables: 7

Abstract

Epidermal growth factor receptor (EGFR) tyrosine kinase inhibitors (TKIs) are the first-line therapies for *EGFR* mutation-positive lung cancer. EGFR-TKIs have favorable therapeutic effects. However, a large proportion of patients with *EGFR* mutation-positive lung cancer subsequently relapse. Some cancer cells survive the initial treatment with EGFR-TKIs, and this initial survival may be associated with subsequent recurrence. Therefore, we aimed to overcome the initial survival against EGFR-TKIs. We hypothesized that yes-associated protein 1 (YAP1) is involved in the initial survival against EGFR-TKIs, and we confirmed the combined effect of EGFR-TKIs and a YAP1–TEAD pathway inhibitor. The KTOR27 (EGFR kinase domain duplication [KDD]) lung cancer cell lines established from a patient with *EGFR* mutation-positive lung cancer and commercially available PC-9 and HCC827 (EGFR exon 19 deletions) lung cancer cell lines were used. These cells were used to evaluate the *in vitro* and *in vivo* effects of VT104, a TEAD inhibitor. Additionally, YAP1 involvement was investigated in pathological specimens. YAP1 was activated by short-term EGFR-TKI treatment in *EGFR* mutation-positive lung cancer cells. In addition, inhibiting YAP1 function using small interfering RNA increased the sensitivity to EGFR-TKIs. Combination therapy with VT104 and EGFR-TKIs showed better tumor-suppressive effects than EGFR-TKIs alone, *in vitro* and

in vivo. Moreover, the combined effect of VT104 and EGFR-TKIs was observed regardless of the localization status of YAP1 before EGFR-TKI exposure. These results suggest that combination therapy with the TEAD inhibitor and EGFR-TKIs may improve the prognosis of patients with *EGFR* mutation-positive lung cancer.

Introduction

Lung cancer is the leading cause of cancer-related deaths worldwide (1), and lung adenocarcinoma is the most common histological type of lung cancer (2). Epidermal growth factor receptor (EGFR) gene mutations are the most frequent driver mutations in lung adenocarcinoma, and approximately half of the patients with lung adenocarcinoma in Asia harbor *EGFR* mutations (3). EGFR-tyrosine kinase inhibitors (TKIs), such as osimertinib, are administered to treat *EGFR* mutation-positive lung cancer and contribute to prolonged survival (4, 5). However, a large proportion of patients with *EGFR* mutation-positive lung cancer subsequently relapse, and a complete cure remains lacking (4).

There are various resistance mechanisms to EGFR-TKIs, such as EGFR secondary mutations, MET amplification, and small cell lung cancer transformation (6). For example, EGFR T790M mutation is a common resistance mechanism to EGFR-TKIs (7) and is treated with osimertinib (8). However, several other resistance mechanisms remain unresolved. These resistance mechanisms complicate overcoming resistance to EGFR-TKIs. Recently, it has been reported that cancer cells that survive initial TKI treatment acquire various resistance mechanisms during subsequent repopulation (9). The involvement of insulin-like growth factor 1 receptor (IGF-1R) signaling and AXL has also been reported as responsible factors defining the initial survival of EGFR-TKIs in

EGFR mutation-positive lung cancer (10, 11); however, the factors responsible for the initial survival are still not fully understood.

Yes-associated protein 1 (YAP1) was isolated in 1995 as a gene encoding a protein that binds to the Src homology 3 domain of the YES proto-oncogene tyrosine kinase (12). YAP1 is a transcriptional cofactor located downstream of the Hippo pathway and is involved in organ size regulation (13). Activated YAP1 translocates to the nucleus and binds to the transcription factor TEAD, inducing expression of genes involved in cell proliferation and survival (14). In addition, YAP1 is activated in many cancers and is associated with anticancer drug resistance (15). Recently, we reported that YAP1 activation is a factor that defines the initial survival of TKIs in anaplastic lymphoma kinase (ALK)-positive and ROS proto-oncogene 1 (ROS1)-positive lung cancers (16, 17). In *EGFR* mutation-positive lung cancer, YAP1 activation also leads to resistance to EGFR-TKIs, and YAP1 inhibition enhances EGFR-TKI sensitivity (18, 19). Therefore, the combination of YAP1 inhibitors and EGFR-TKIs is a useful therapeutic strategy to overcome EGFR-TKI resistance, but the lack of clinically applicable YAP1 inhibitors remains a problem to be solved.

Several preclinical studies have been conducted using YAP1–TEAD inhibitors in *EGFR* mutation-positive lung cancers. For example, in preclinical studies, verteporfin,

a YAP1–TEAD inhibitor, was used to inhibit the YAP1–TEAD pathway in *EGFR* mutation-positive lung cancer (20, 21). However, it is not used clinically to treat cancers, including lung cancer. Side effects such as photosensitivity may make it challenging to use verteporfin clinically. Similarly, CA3 and K-975 were used as YAP1–TEAD pathway inhibitors in preclinical studies on esophageal cancer and malignant pleural mesothelioma (22, 23). Moreover, MYF-01-37, a TEAD inhibitor, has been developed; it enhanced apoptosis when used in combination with EGFR-TKIs and MEK inhibitors in *EGFR* mutation-positive lung cancer (24). However, these drugs are currently not used clinically.

VT104 and VT103 were developed as selective inhibitors of TEAD auto-palmitoylation and showed antitumor activity against *NF2*-deficient malignant pleural mesothelioma (25). The TEAD transcription factor family includes four known types, TEAD1–4, particularly significant in mammalian development (26). VT104 is characterized by its ability to inhibit TEAD1–4 (25). In contrast, VT103 primarily inhibits TEAD1 (25). Although studies using other TEAD inhibitors have been reported, these TEAD inhibitors have short half-lives and require high doses *in vivo* (27). However, VT104 has a favorable oral bioavailability and a long half-life (25). VT3989, which is mechanistically very similar to VT104, shows similar biological activity *in vitro* and *in vivo* (28). VT3989 is safe and well tolerated and has demonstrated durable anti-tumor

activity in patients with advanced mesothelioma with or without NF2 mutations and in other solid tumors with NF2 mutations (28). Hence, VT104 is one of the YAP1−TEAD inhibitors that are expected to be applied clinically in the future.

We hypothesized that the combination of VT104 and EGFR-TKIs would be a clinically applicable treatment strategy for *EGFR* mutation-positive lung cancer that inhibits initial survival against EGFR-TKIs. We aimed to evaluate the efficacy of the combination of VT104 and EGFR-TKIs on *EGFR* mutation-positive lung cancer *in vitro* and *in vivo*. In addition, we examined whether the combination of VT104 and EGFR-TKI is beneficial regardless of the cellular localization status of YAP1 prior to EGFR-TKI exposure.

Materials and Methods

Clinical information and informed consent procedures

The study protocol was prepared following the Declaration of Helsinki and was approved by the Ethics Committee of Kyoto University Graduate School and Faculty of Medicine (Kyoto, Japan; certification number: R2163). The clinical information of the patient was obtained from electronic medical records. In addition, the patient provided written informed consent to participate in this study.

Establishment of patient-derived cell lines

The KTOR27 (EGFR kinase domain duplication [KDD]) lung cancer cell line was established from a patient with *EGFR* mutation-positive lung cancer who regularly visited the Kyoto University Hospital (Kyoto, Japan). The patient was diagnosed with lung adenocarcinoma, and next-generation sequencing by FoundationOne® CDx (Foundation Medicine, Inc., Cambridge, Massachusetts, United States) revealed a duplication of EGFR exons 18–25, called EGFR-KDD. The patient was initiated with afatinib treatment; however, the left pleural effusion worsened approximately 2 months after the initiation. The malignant pleural effusion used to establish the cell line was collected when the left pleural effusion worsened (Fig. 1A). Patient-derived cells were established as described previously (29). Briefly, the pleural effusion of the patient was centrifuged to separate the tumor cells. The tumor cells were maintained in RPMI1640 medium (Nacalai Tesque, Kyoto, Japan) supplemented with 8% heat-inactivated fetal bovine serum (Sigma-Aldrich, St. Louis, Missouri, United States) and 1% penicillin/streptomycin (Gibco, Waltham, Massachusetts, United States) at 37.0 °C in 5% CO_2.

Cell lines and reagents

The PC-9 (EGFR exon 19 deletion) lung cancer cell line was purchased from the European Collection of Authenticated Cell Cultures (Porton Down, UK) in 2014. The HCC827 (EGFR exon 19 deletion) and H1975 (EGFR exon 21 L858R mutation and EGFR exon 20 T790M mutation) lung cancer cell lines were purchased from the American Type Culture Collection (Manassas, Virginia, United States) in 2016 and 2023, respectively. These cells were used within 2 months after thawing. In 2023, these cells were confirmed to be negative for Mycoplasma using the MycoAlert Mycoplasma Detection Kit (Lonza, Basel, Switzerland). Osimertinib was purchased from ChemScene, LLC (Monmouth Junction, New Jersey, United States). Afatinib and alectinib were purchased from LC Laboratories (Woburn, Massachusetts). Verteporfin was purchased from Cayman Chemical Company (Ann Arbor, Michigan, United States). VT104 and VT103 were provided by Vivace Therapeutics, Inc. (San Mateo, California, United States). Osimertinib, afatinib, alectinib, VT104, and VT103 were dissolved in dimethyl sulfoxide (DMSO; Nacalai Tesque, Kyoto, Japan). DMSO was used as the vehicle control.

Cell viability and drug sensitivity assays

Cells (3,000–5,000 cells/well) were cultured overnight in 96-well plates. All

plates were incubated the following day with stepwise concentrations of the indicated reagents. After 3–7 days of incubation, viable cell counting was performed using the CellTiter-Glo 2.0 assay (Promega, Madison, Wisconsin, United States). Luminescence was measured using ARVO X3 (PerkinElmer, Waltham, Massachusetts, United States), and half maximal inhibitory concentrations (IC_{50}) were calculated with nonlinear regression models with sigmoidal dose responses using GraphPad Prism 9 (GraphPad Software, La Jolla, California, United States).

Cell growth assays

Cell growth assays were performed following previous reports (29, 30). Cells (5,000 cells/well) were cultured overnight in 96-well plates. The following day, all plates were incubated with the indicated reagent concentration. One plate was immediately frozen (−80 °C) as a baseline. After 24–72 h of incubation, the remaining plates were frozen (−80 °C). Plates were thawed simultaneously, and viable cells were counted using the CellTiter-Glo 2.0 assay and ARVO X3. The relative cell counts compared with the baseline plate were calculated. We confirmed that a single freezing and thawing procedure for the cells had a minimal effect on the CellTiter-Glo luminescence signals (Supplementary Fig. S1).

Apoptosis assays

Cells (1,500–5,000 cells/well) were cultured in 384-well plates overnight and incubated with the indicated reagents for 24 h. Caspase 3/7 activity was assessed using the Caspase-Glo 3/7 assay (Promega) according to the manufacturer's protocol. The measured value was normalized according to the cell number using the CellTiter-Glo 2.0 assay.

Immunoblotting

SDS-PAGE and immunoblotting were performed as previously described (31). Information on the primary antibodies used in this study is summarized in Supplementary Table S1. Secondary antibodies used in this study were purchased from Cell Signaling Technology (Danvers, Massachusetts, United States). Primary and secondary antibodies were diluted in 2.5% bovine serum albumin (BSA) (Nacalai Tesque)/Tris-buffered saline containing Tween 20 (TBS-T).

Immunofluorescence staining

The cells were fixed with 4% paraformaldehyde in phosphate-buffered saline

(PBS) (Nacalai Tesque) for 20 min and permeabilized with 0.2% Triton X-100 in PBS for 15 min. Subsequently, the cells were blocked with PBS supplemented with 5% (w/v) normal donkey serum (Merck Millipore, Burlington, Massachusetts, United States) and 1% (w/v) BSA (Sigma-Aldrich) for 30 min. Furthermore, the cells were incubated overnight with the primary antibody solution at 4 °C. The next day, the cells were incubated with the secondary antibody solution for 30 min at 25 °C. Finally, immunofluorescently-labeled cells were photographed under a BZ-710 microscope (KEYENCE, Osaka, Japan). The percentage of cells with YAP1 nuclear localization was calculated using the following formula: (the number of cells with YAP1 nuclear localization/the total number of cells) × 100 . The primary antibodies used in this study are listed in Supplementary Table S2.

Quantitative reverse transcription-PCR (qRT-PCR)

Total RNA was extracted from cultured cells using a PureLink® RNA Mini Kit (Thermo Fisher Scientific, Waltham, Massachusetts, United States). Gene expression was measured through qRT-PCR using 100 ng of total RNA, One Step TB Green® PrimeScript RT-PCR Kit II (Takara Bio, Shiga, Japan), and primer pairs. The list of the primer pairs purchased from Thermo Fisher Scientific is shown in Supplementary Table S3. Reactions

were quantified using the QuantStudio™ 3 Real-Time polymerase chain reaction System (Applied Biosystems, Foster City, California, United States).

Transfection with small interfering RNAs (siRNAs)

The siRNA oligonucleotides for *YAP1* and the negative control were purchased from Thermo Fisher Scientific (Stealth RNAi™ or Silencer® Select siRNA, Supplementary Table S4). Cells ($3.0–5.0 \times 10^5$) were transfected with siRNA oligonucleotides at a final RNA concentration of 20 or 5 nmol/L using Lipofectamine® RNAiMAX Transfection Reagent (Invitrogen, Waltham, Massachusetts, United States). Reverse transfection was performed according to the manufacturer's instructions.

Compound library screening

A compound library containing approximately 1,800 compounds was provided by the Center for Drug Discovery Research, Kyoto University (Kyoto, Japan). The compounds were diluted in DMSO. The cells (800 cells/well) were cultured in 384-well plates overnight. The next day, all plates were incubated with 150 nM osimertinib and 10 μM library compounds. After 3 days of incubation, viable cell counts were measured using the CellTiter-Glo 2.0 assay and ARVO X3. Relative cell counts were calculated and

compared with those of cells exposed to osimertinib alone.

Patient selection and assessment of clinical outcomes

Patients diagnosed with *EGFR* mutation-positive lung cancer who underwent surgery at the Kyoto University Hospital between 2002 and 2009 were included in the tissue microarray (TMA) analysis. An expert pathologist (A.Y.) reviewed and confirmed the pathological diagnosis of consecutive lung adenocarcinomas to prepare the TMAs. Forty-two patients were included in this study. Progression-free survival (PFS) was measured from the initiation of the EGFR-TKI therapy until the date of disease progression or death. The study protocol was prepared following the Declaration of Helsinki and was approved by the Kyoto University Graduate School and Faculty of Medicine Ethics Committee (certification number: R0854).

Immunohistochemistry and image analysis

The procedures for immunohistochemistry and image analysis have been previously described in detail (32). The concentrations of the primary antibodies used are listed in Supplementary Table S5. Immunohistochemical staining for YAP1 was performed using Ventana Discovery Ultra (Roche, Tucson, Arizona, United States).

Antigen-antibody reactions were observed using the Ventana UltraView Universal DAB Detection Kit (Roche). All stained slides were digitized using a NanoZoomer S360 digital slide scanner (Hamamatsu Photonics, Hamamatsu, Japan). Analyses were performed using the HALO image analysis software (Indica Labs, Albuquerque, New Mexico, United States). The positivity threshold for staining was determined empirically based on the controls, and the intensity was classified from 0 to 3. The H-score was calculated using the following formula: (1% weakly positive cells) + (2% moderately positive cells) + (3% strongly positive cells) according to the HALO configuration settings (Supplementary Table S6). The nuclear localization of YAP1 was defined as nuclear optical density (OD) of YAP1 > cytoplasmic OD of YAP1.

Xenograft models

Six-week-old female BALB/c-nu (CAnN.Cg-Foxn1nu/CrlCrlj) and SHO mice (Crlj: SHO-PrkdcscidHrhr) were purchased from Charles River Laboratories (Yokohama, Japan). To generate xenograft models, PC-9 and HCC827 cells ($3.0–5.0 \times 10^6$) were suspended in Matrigel® (Corning, Corning, New York, United States) and injected subcutaneously into the flanks of the mice. Tumor width and length were measured every 3 days using digital calipers. Tumor volumes were calculated using the following

formula: (length × width^2) × 0.51. When the tumor volumes reached approximately 150–200 mm^3, the mice were randomly assigned to each treatment group, and the treatment was initiated. All animal experiments and research plans were approved by the Animal Research Committee of Kyoto University (Kyoto, Japan; ID: MedKyo 22519) and performed following the ARRIVE guidelines.

Statistical analysis

Continuous variable data are expressed as the mean ± SEM. The significant differences between the two groups were compared using Student's *t*-test. The significant differences between three or more groups were compared using one-way ANOVA, followed by Dunnett's or Sidak's multiple comparison test. PFS curves were constructed using the Kaplan–Meier method and compared using the log-rank test. The *p*-values of <0.05 were considered significant. Statistical analyses and visualization were performed using GraphPad Prism 9 and JMP Pro statistical software version 15.2.0 (SAS Institute, Cary, North Carolina, United States).

Data availability

The data analyzed in this study are available from the corresponding author upon request.

Results

Establishment of a patient-derived *EGFR* mutation-positive lung cancer cell line (KTOR27)

We established a cell line (KTOR27) using the malignant pleural effusion derived from a patient with *EGFR* mutation-positive lung cancer. In this case, afatinib treatment was ineffective. Therefore, we established a cell line from the malignant pleural effusion of the patient after the disease progression with afatinib treatment. Using immunoblotting *in vitro*, EGFR-KDD was confirmed by its high molecular weight compared with that of wild-type EGFR or those of other common *EGFR* mutations, such as EGFR exon 19 deletions (33, 34). Therefore, we performed immunoblotting to confirm the molecular weight of EGFR in the KTOR27 cells. The KTOR27 cells harbored a higher molecular weight of EGFR than PC9 and HCC827 cells harboring EGFR exon 19 deletions (Fig. 1B). These results indicate that the KTOR27 cells had EGFR-KDD.

YAP1 is activated by afatinib treatment in KTOR27 cells

Osimertinib is the most commonly used first-line treatment in patients with *EGFR* mutation-positive lung cancer. However, *EGFR* mutation-positive lung cancer

cells with EGFR-KDD are more sensitive to afatinib than to osimertinib (33). Similarly, KTOR27 cells were more sensitive to afatinib than to osimertinib (Fig. 1C). The IC_{50} values for afatinib and osimertinib treatments of KTOR27 cells were 10.5 and 96.3 nmol/L, respectively. Although it was assumed that KTOR27 cells would be resistant to afatinib based on the patient's clinical course, the *in vitro* results showed that KTOR27 cells were sensitive to afatinib. We hypothesized that KTOR27 cells had not acquired complete tolerance to afatinib owing to its lower translocation into the thoracic cavity compared to the bloodstream, which reduced its cytotoxic effect. Another possible reason is that the patient's overall condition was already poor at the initiation of afatinib treatment and the tumor may have further deteriorated before afatinib could take effect. In fact, the patient passed away two months after initiating afatinib treatment, indicating the possibility of a poor prognosis at the time of afatinib initiation. In addition, we investigated whether afatinib suppressed EGFR phosphorylation in KTOR27 cells. Cells were exposed to afatinib at increasing concentrations, and EGFR phosphorylation was evaluated using immunoblotting. EGFR phosphorylation in KTOR27 cells was sufficiently suppressed by afatinib at concentrations close to its IC_{50} value (Fig. 1D). To investigate whether YAP1 was involved in the initial survival mechanism of afatinib-treated KTOR27 cells, we examined whether afatinib treatment induced YAP1 activation.

In KTOR27 cells, YAP1 was localized in the cytoplasm without afatinib exposure and in the nucleus after 72 h of exposure (Fig. 2A). The percentage of cells with YAP1 nuclear localization increased considerably in the afatinib-treated KTOR27 cells (Fig. 2B).

Inhibition of YAP1–TEAD increases the sensitivity of KTOR27 cells to afatinib

YAP1 expression was inhibited in KTOR27 cells to evaluate the function of YAP1 in cancer cell survival against afatinib. Transfection of siRNA targeting *YAP1* into KTOR27 cells decreased *YAP1* expression (Fig. 2C). We performed cell viability assays after afatinib treatment in *EGFR* mutation-positive lung cancer cells with the gene inhibition of *YAP1*. *YAP1* inhibition significantly reduced the survival rate of KTOR27 cells under afatinib treatment (Fig. 2C). Next, we used TEAD inhibitors, VT103 and VT104, against the YAP1–TEAD pathway. First, we performed cell viability assays for KTOR27 cells exposed to VT103 or VT104 and found that neither compound, as monotherapy, exerted any considerable effects on KTOR27 cell viability at a concentration of less than 10 μM (Supplementary Fig. S2). We then performed cell viability assays for KTOR27 cells exposed to afatinib in combination with either VT103 or VT104 (Fig. 2D and Supplementary Fig. S3). Although combination therapy with afatinib and VT103 or VT104 was more effective than afatinib alone, VT104 was more

effective in combination with afatinib than VT103 (Fig. 2D and Supplementary Fig. S3). Therefore, VT104 was used in subsequent experiments. In addition, we performed cell viability assays for KTOR27 cells treated with osimertinib and VT104 (Fig. 2D). The combination effect of osimertinib and VT104 was observed in KTOR27 cells; however, afatinib showed a more substantial combined effect with VT104 than did osimertinib (Fig. 2D). VT103 and VT104 significantly enhance the sensitivity of EGFR-TKIs in a concentration range where VT103 and VT104 monotherapy show limited efficacy in KTOR27 cells. Therefore, VT103 and VT104 show synergistic effects with EGFR-TKIs in KTOR27 cells. Furthermore, we performed cell viability assays for KTOR27 cells treated with afatinib and verteporfin (Supplementary Fig. S4). The combination effect of afatinib and verteporfin was observed in KTOR27 cells. However, VT104 showed a more substantial combined effect with afatinib than did verteporfin (Fig. 2D and Supplementary Fig. S4). Combination therapy with afatinib and VT104 significantly increased caspase 3/7 activity compared with afatinib alone (Fig. 2E). The caspase 3/7 activity of VT104 alone was reduced compared with that of the vehicle. Thus, VT104 enhanced apoptosis only when combined with afatinib. To evaluate YAP1 transcriptional activation, *CTGF* expression was assessed. *CTGF* expression increased under afatinib treatment, and the afatinib-induced activation of *CTGF* expression decreased in the

presence of VT104 (Fig. 2F). In addition, *CYR61* expression increased under afatinib treatment, and the afatinib-induced activation of *CYR61* expression decreased in the presence of VT104 (Supplementary Fig. S5). *YAP1* inhibition decreased *CTGF* expression (Supplementary Fig. S6). In contrast, *TEAD1* inhibition did not decrease *CTGF* expression (Supplementary Fig. S7). In addition, the depletion of *TEAD1* with siRNA did not change the KTOR27 response to afatinib in cell growth assays (Supplementary Fig. S8). Taken together, these data suggest that other TEAD family members (TEAD2, TEAD3, and/or TEAD4) are necessary for the YAP1-mediated survival mechanism in KTOR27 cells in response to afatinib treatment. This is consistent with the finding that VT103, a TEAD1-selective inhibitor, is not as effective as VT104, that inhibits more than TEAD1, in enhancing the potency of afatinib in KTOR27 cells.

YAP1 is activated under osimertinib treatment in PC9 and HCC827 cells

Next, we investigated the mechanisms involved in the initial survival against EGFR-TKIs in *EGFR* mutation-positive lung cancer cells other than KTOR27 cells. We used PC9 and HCC827 cells and osimertinib as an EGFR-TKI for these cells. First, to identify compounds that can enhance osimertinib efficacy in PC9 cells, we performed high-throughput compound screening using a compound library of approximately 1,800

compounds. The relative cell viability rates resulting from the combination of these library compounds with osimertinib in PC9 cells are presented in Supplementary Data S1. Remarkably, verteporfin and cerivastatin, acting as YAP1 inhibitors, were identified in the top 100 most effective library compounds (Fig. 3A). This finding suggests that YAP1–TEAD inhibitors might be as effective or more effective in combination with EGFR inhibitors than other compounds in inhibiting the initial survival of *EGFR* mutation-positive lung cancer. Therefore, to determine whether activation of YAP1 mediating cell survival in afatinib-treated KTOR27 cells also occurs in other *EGFR*-mutated lung cancer cells in response to other EGFR-TKIs, we performed similar experiments using PC9 and HCC827 cells. PC9 and HCC827 cells exhibited adequate sensitivity to osimertinib (Fig. 3B). The IC_{50} values of osimertinib in PC9 and HCC827 cell viability assays were 123 and 379 nmol/L, respectively. The IC_{50} values in our study are higher than those previously reported (35, 36). We considered that potential factors, such as differences in cell preservation methods, culture conditions, and duration of osimertinib exposure, may contribute to the discrepancy in these IC_{50} values. We investigated whether osimertinib suppresses EGFR phosphorylation in PC9 and HCC827 cells. Osimertinib was administered in dose titration, and EGFR phosphorylation was evaluated using immunoblotting. EGFR phosphorylation in PC9 and HCC827 cells was sufficiently

suppressed by osimertinib at concentrations close to the respective IC_{50} values (Fig. 3C). Next, we evaluated YAP1 activation by osimertinib in PC9 and HCC827 cells. In PC-9 cells without osimertinib exposure, YAP1 was localized in the cytoplasm. However, YAP1 was localized in the nucleus after osimertinib exposure for 72 h (Fig. 3D). YAP1 was initially localized in the nucleus of HCC827 cells without osimertinib exposure, and the nuclear localization of YAP1 was maintained after osimertinib exposure for 72 h (Fig. 3E). The percentage of cells with YAP1 nuclear localization increased considerably in osimertinib-treated PC9 cells (Fig. 3F); however, there was no such notable difference in that of osimertinib-treated HCC827 cells (Fig. 3F).

Inhibition of YAP1 increases the sensitivity to osimertinib in PC9 and HCC827 cells

YAP1 expression was inhibited in PC9 and HCC827 cells to evaluate the role of YAP1 in cancer cell survival in response to osimertinib. The transfection of siRNA targeting *YAP1* into these cells reduced *YAP1* expression (Fig. 4A). Subsequently, we performed cell viability assays after osimertinib exposure in PC9 and HCC827 cells with the *YAP1* gene inhibition. *YAP1* inhibition significantly reduced the survival rates of PC9 and HCC827 cells after osimertinib treatment (Fig. 4B). Next, we performed cell viability assays for VT104 exposure in PC9 and HCC827 cells. In these cells, the VT104

monotherapy was ineffective (Supplementary Fig. S9). Subsequently, we performed cell viability assays with osimertinib in PC9 and HCC827 cells exposed to VT104. The combination therapy of osimertinib and VT104 was more effective than osimertinib monotherapy (Fig. 4C). VT104 significantly enhances the sensitivity of osimertinib in a concentration range where VT104 monotherapy shows limited efficacy in PC9 and HCC827 cells. Therefore, VT104 shows synergistic effects with osimertinib in PC9 and HCC827 cells. Furthermore, combination therapy with osimertinib and VT104 significantly increased caspase 3/7 activity compared with osimertinib alone in PC9 and HCC827 cells (Fig. 4D). In addition, *CTGF* expression was increased by osimertinib and decreased by combination therapy of osimertinib and VT104 (Fig. 4E). The combination effect of VT104 and osimertinib was also assessed in H1975 cells. In H1975 cells, while the VT104 monotherapy was ineffective (Supplementary Fig. S9), the combination therapy of osimertinib and VT104 was more effective than osimertinib monotherapy (Supplementary Fig. S10). In addition, YAP1 was localized in the cytoplasm in H1975 cells without osimertinib exposure (Supplementary Fig. S11). However, YAP1 was localized in the nucleus after osimertinib exposure for 72 h (Supplementary Fig. S11). The percentage of cells with YAP1 nuclear localization increased considerably in osimertinib-treated H1975 cells (Supplementary Fig. S11). These findings may indicate

that YAP1 is potentially also involved in the initial survival against osimertinib in H1975 cells.

Combination therapy with osimertinib and VT104 inhibits tumor regrowth of PC9 and HCC827 cells *in vivo*

Based on these *in vitro* results, we confirmed the combined effects of osimertinib and VT104 *in vivo*. Because we could not establish xenograft models using KTOR27 cells, xenograft models using PC-9 or HCC827 cells were established and used for *in vivo* testing. The tumor-bearing mice were randomized into four groups as follows: vehicle, VT104 monotherapy, osimertinib monotherapy, and combination therapy with osimertinib and VT104 (Fig. 5A). Each group received the assigned treatment for 2 weeks and was monitored for tumor volume during and after treatment (Fig. 5A). Based on previous reports, the osimertinib dose was 5 mg/kg (11, 37), and the VT104 dose was 10 mg/kg (25). The osimertinib monotherapy group showed a relatively fast rate of tumor regrowth after discontinuing osimertinib (Fig. 5B and C). In contrast, the osimertinib and VT104 combination therapy group showed a slower tumor regrowth rate after discontinuing the combination therapy than the osimertinib monotherapy group (Fig.5B and C). VT104 monotherapy had no apparent tumor-suppressive effect compared with

the vehicle in PC-9 and HCC827 cells (Fig. 5B and C). The tumor volumes of PC-9 and HCC827 cells on the last day of observation (36 and 63 days, respectively) were significantly lower in the osimertinib and VT104 combination therapy group than in the osimertinib monotherapy group (Fig. 5D). Furthermore, combination therapy with osimertinib and VT104 did not worsen the rate of weight loss compared with osimertinib monotherapy in PC-9 and HCC827 cells (Fig. 5B and C).

Association between the clinical outcomes and immunohistochemical YAP1 expression in TMA

The role of YAP1 in clinical practice was investigated by evaluating the association between the clinical outcomes of EGFR-TKIs and immunohistochemical YAP1 expression using TMA of *EGFR* mutation-positive lung cancers (Fig. 6A). Patient characteristics are presented in Supplementary Table S7. Thirty-one of 42 patients were treated with EGFR-TKIs. There was no significant difference in PFS between patients with YAP1 nuclear localization and YAP1 cytoplasmic localization (22.4 months versus 33.2 months; $p = 0.48$; Fig. 6B). This result differs from our finding that YAP1 nuclear localization attenuated the therapeutic effect of EGFR-TKIs *in vitro*. We considered the possibility that this discrepancy may have occurred because the majority of lung cancers

in our TMA are at stages I to III, and the YAP1 nuclear localization status may differ from that of stage IV or recurrent cancers that are treated with EGFR-TKIs from the beginning.

Discussion

In this study, we found that combining an EGFR-TKI and VT104, a TEAD inhibitor, effectively promoted the apoptosis of *EGFR* mutation-positive lung cancer cells and delayed tumor regrowth after treatment by inhibiting the activation of the YAP1–TEAD pathway (Fig. 6C). In addition, this is the first study to demonstrate that activating the YAP1–TEAD pathway determines the initial survival of *EGFR* mutation-positive lung cancer cells, regardless of the subcellular localization status of YAP1 before treatment initiation.

The involvement of IGF-1R signaling and AXL is reportedly an early survival mechanism of EGFR-TKIs in *EGFR* mutation-positive lung cancer (10, 11). In this study, YAP1 was localized in the cytoplasm before EGFR-TKI treatment in PC-9 and KTOR27 cells; however, YAP1 migrated into the nucleus upon EGFR-TKI treatment (Fig. 2A and Fig. 3D). Furthermore, in PC-9 and KTOR27 cells, suppressing *YAP1* expression and inhibiting TEAD using VT104 increased sensitivity to EGFR-TKIs, suggesting that YAP1 activity may be a factor defining early survival after EGFR-TKI treatment. These results

are supported by the fact that verteporfin and cerivastatin, which inhibit YAP1 activity, were effective in PC-9 cells in the library compounds tested for their efficacy in combination with osimertinib. This is consistent with our previous report showing that YAP1 activity is an early survival determinant of TKI in ALK-positive and ROS1-positive lung cancers (16, 17). This suggests that YAP1 activity may be involved in the initial survival of multiple molecularly-targeted therapies, regardless of the type of mutation.

In contrast, HCC827 cells contained YAP1 in the nucleus before EGFR-TKI treatment, and YAP1 remained in the nucleus after EGFR-TKI treatment. Thus, in *EGFR* mutation-positive lung cancer cells, YAP1 has two different localization states before EGFR-TKI exposure, in the cytoplasm and nucleus. In HCC827, PC-9, and KTOR27 cells, inhibition of the YAP1–TEAD pathway enhanced sensitivity to EGFR-TKIs and delayed tumor regrowth. In addition, EGFR-TKI exposure increased *CTGF* expression downstream of the YAP1–TEAD pathway, suggesting that TKI exposure activated the YAP1–TEAD pathway in HCC827 cells. These results suggest that in *EGFR* mutation-positive lung cancer cells, activating the YAP1–TEAD pathway is associated with cell survival during the early phase of therapy, regardless of the localization status of YAP1. These results suggest that combination therapy with EGFR-TKIs and TEAD inhibitors benefits both types of YAP1 localization in *EGFR* mutation-positive lung cancers. We

believe that these findings are essential for future clinical applications.

YAP1 levels before treatment are reportedly a poor prognostic factor in non-small cell lung cancer (38), and patients with high nuclear YAP1 levels before EGFR-TKI treatment have a poor prognosis (39). These results are consistent with the *in vitro* experiments in the present study in which osimertinib sensitivity was lower in HCC827 cells than in PC9 cells. Furthermore, *EGFR* mutation-positive lung cancer cells that acquired resistance to EGFR-TKI had nuclear-localized YAP1, and combination therapy with EGFR-TKI and a YAP1 inhibitor was effective (20). Thus, it is likely that the nuclear localization of YAP1 attenuates the therapeutic effect of EGFR-TKIs. However, the results using TMA in this study showed no significant difference in PFS between patients with YAP1 nuclear localization and YAP1 cytoplasmic localization (22.4 months versus 33.2 months; $p = 0.48$; Fig. 6B). This finding differs from the previous report, where high nuclear YAP1 levels before EGFR-TKI treatment were associated with a poor prognosis (39). This inconsistency may be due to different patient populations and the small number of studies compared with previous reports. On the other hand, lung cancers with YAP1 localized in the cytoplasm before EGFR-TKI treatment may also have tumor cell survival in the early stages of treatment owing to YAP1 migration into the nucleus, likely induced by EGFR-TKI treatment. Thus, regardless of the pretreatment localization of YAP1,

combining EGFR-TKIs and TEAD inhibitors may prolong PFS in patients with *EGFR* mutation-positive lung cancer. Since accurate assessment of YAP1 localization in real-world clinical practice is challenging given the differences in specimen types and specimen storage methods among institutions, we believe that combination therapy with EGFR-TKIs and TEAD inhibitors is indicated for all patients with *EGFR* mutation-positive lung cancer.

CTGF is a direct target gene of the YAP1–TEAD pathway (40) and is often used to inform transcriptional activation of YAP1 (41). In this study, we demonstrated that VT104 inhibits the YAP1–TEAD pathway in combination with EGFR-TKIs by confirming a decrease in *CTGF* expression. The decrease in *CTGF* expression was confirmed by YAP1 inhibition through siRNA, not TEAD1 inhibition. These results suggest that TEAD1 inhibition alone may have a weak inhibitory effect on the YAP1–TEAD pathway. These results may also explain why VT104 was more effective in combination with EGFR-TKI than VT103 in this study. Furthermore, combination therapy with VT104 and EGFR-TKIs did not worsen weight loss compared with osimertinib monotherapy *in vivo*. In previous studies, the IC_{50} of VT104 for the *NF2*-deficient malignant pleural mesothelioma cell line NCI-H226 was relatively low at 16.1 nmol/L, and the steady-state volume of distribution of VT104 at 9.55 mg/kg intravenous

injection was 3.64 L/kg (25). Additionally, the half-life of VT104 after oral administration at a dose of 9.55 mg/kg was 30.74 h (25). These results indicate that VT104 is able to inhibit tumor growth at low doses *in vivo* (25), and that VT104 may be well tolerated in combination with EGFR-TKIs.

This study had some limitations. First, we performed *in vivo* experiments using only two *EGFR* mutation-positive lung cancer cell lines (both harboring EGFR exon 19 deletions). The effects of EGFR-TKI may vary depending on the *EGFR* mutation subtype (5). Therefore, *in vivo* experiments should be performed using other *EGFR* mutations, including L858R. Second, we did not show factors regulated by the YAP1–TEAD pathway that mediate the survival mechanisms. YAP1–TEAD transcribes genes significant in cancer cell growth, such as *Sox2*, *Snai2*, and *AXL* (42). Future studies are needed to determine which factors downstream of the YAP1–TEAD pathway are activated and which exert survival effects in the presence of EGFR-TKI treatment. Third, we could not confirm whether the YAP1–TEAD pathway was activated by the binding of YAP1 to TEAD in HCC827 cells, where YAP1 was localized in the nucleus before treatment. In contrast, we confirmed that the YAP1–TEAD pathway was activated in HCC827 cells following EFGR-TKI treatment. However, the significance of this study is that the combined effect of EGFR-TKI and TEAD inhibitors was demonstrated regardless

of the YAP1 localization status before EGFR-TKI treatment.

This study showed that combination therapy with EGFR-TKIs and VT104 aids in treating *EGFR* mutation-positive lung cancer. Unlike previous agents that inhibit the YAP1–TEAD pathway, VT104 may be well tolerated, and we believe that the combination therapy of EGFR-TKI and VT104 is a new therapeutic strategy with the potential for future clinical application. Furthermore, because the combination therapy of EGFR-TKIs and VT104 is independent of the pretreatment YAP1 localization status, it should contribute to improving the prognosis of more patients with *EGFR* mutation-positive lung cancer, which is an essential preclinical study for its clinical application.

Acknowledgments

We thank Tracy T. Tang from Vivace Therapeutics Inc. for providing us with VT104 and VT103, developed by their company, and for proofreading and valuable comments for this paper. We also thank the Center for Anatomical, Pathological, and Forensic Medical Research, Graduate School of Medicine, Kyoto University, for preparing the microscope slides. Furthermore, we thank Yukiko Okuno, Center for Drug Discovery Research, Kyoto University, for her assistance with compound library screening. Finally, we thank Yuko Maeda from the Department of Respiratory Medicine, Graduate School of Medicine,

Kyoto University, for her assistance with the experiments.

Author contributions

T. Ogimoto and H. Ozasa conceived and designed this study. T. Ogimoto conducted experiments. T. Ogimoto and H. Ozasa analyzed the data. A. Yoshizawa immunohistochemically evaluated TMAs. T. Ogimoto drafted the manuscript. All authors contributed to data interpretation, discussion, and final approval of the manuscript.

References

1. Sung H, Ferlay J, Siegel RL, Laversanne M, Soerjomataram I, Jemal A, et al. Global Cancer Statistics 2020: GLOBOCAN Estimates of Incidence and Mortality Worldwide for 36 Cancers in 185 Countries. *CA Cancer J Clin* **2021**;71:209−49.

2. Youlden DR, Cramb SM, Baade PD. The International Epidemiology of Lung Cancer: geographical distribution and secular trends. *J Thorac Oncol* **2008**;3:819−31.

3. Midha A, Dearden S, McCormack R. EGFR mutation incidence in non-small-cell lung cancer of adenocarcinoma histology: a systematic review and global map by ethnicity (mutMapII). *Am J Cancer Res* **2015**;5:2892−911.

4. Soria JC, Ohe Y, Vansteenkiste J, Reungwetwattana T, Chewaskulyong B, Lee KH, et al. Osimertinib in Untreated EGFR-Mutated Advanced Non-Small-Cell Lung Cancer. *N Engl J Med* **2018**;378:113−25.

5. Ramalingam SS, Vansteenkiste J, Planchard D, Cho BC, Gray JE, Ohe Y, et al. Overall Survival with Osimertinib in Untreated, EGFR-Mutated Advanced NSCLC. *N Engl J Med* **2020**;382:41−50.

6. Leonetti A, Sharma S, Minari R, Perego P, Giovannetti E, Tiseo M. Resistance mechanisms to osimertinib in EGFR-mutated non-small cell lung cancer. *Br J Cancer* **2019**;121:725−37.

7. Sequist LV, Waltman BA, Dias-Santagata D, Digumarthy S, Turke AB, Fidias P, et al. Genotypic and histological evolution of lung cancers acquiring resistance to EGFR inhibitors. *Sci Transl Med.* **2011**;3:75ra26.

8. Mok TS, Wu Y-L, Ahn M-J, Garassino MC, Kim HR, Ramalingam SS, et al. Osimertinib or Platinum-Pemetrexed in EGFR T790M-Positive Lung Cancer. *N Engl J Med.* **2017**;376:629−40.

9. Lin JJ, Shaw AT. Resisting Resistance: Targeted Therapies in Lung Cancer. *Trends Cancer* **2016**;2:350−64

10. Sharma SV, Lee DY, Li B, Quinlan MP, Takahashi F, Maheswaran S, et al. A chromatin-mediated reversible drug-tolerant state in cancer cell subpopulations. *Cell* **2010**;141:69−80.

11. Taniguchi H, Yamada T, Wang R, Tanimura K, Adachi Y, Nishiyama A, et al. AXL confers intrinsic resistance to osimertinib and advances the emergence of tolerant cells. *Nat Commun* **2019**;10:259.

12. Sudol M, Bork P, Einbond A, Kastury K, Druck T, Negrini M, et al. Characterization of the mammalian YAP (Yes-associated protein) gene and its role in defining a novel protein module, the WW domain. *J Biol Chem* **1995**;270:14733−41.

13. Yu FX, Zhao B, Guan KL. Hippo Pathway in Organ Size Control, Tissue Homeostasis,

and Cancer. *Cell* **2015**;163:811−28.

14. Moroishi T, Hansen CG, Guan KL. The emerging roles of YAP and TAZ in cancer. *Nat Rev Cancer* **2015**;15:73−9.

15. Zanconato F, Cordenonsi M, Piccolo S. YAP/TAZ at the Roots of Cancer. *Cancer Cell* **2016**;29:783−803.

16. Tsuji T, Ozasa H, Aoki W, Aburaya S, Yamamoto Funazo T, Furugaki K, et al. YAP1 mediates survival of ALK-rearranged lung cancer cells treated with alectinib via pro-apoptotic protein regulation. *Nat Commun* **2020**;11:74.

17. Yamazoe M, Ozasa H, Tsuji T, Funazo T, Yoshida H, Hashimoto K, et al. Yes-associated protein 1 mediates initial cell survival during lorlatinib treatment through AKT signaling in ROS1-rearranged lung cancer. *Cancer Sci.* **2023**;114:546−60.

18. Hsu PC, You B, Yang YL, Zhang WQ, Wang YC, Xu Z, et al. YAP promotes erlotinib resistance in human non-small cell lung cancer cells. *Oncotarget* **2016**;7:51922−33.

19. Huang JM, Nagatomo I, Suzuki E, Mizuno T, Kumagai T, Berezov A, et al. YAP modifies cancer cell sensitivity to EGFR and survivin inhibitors and is negatively regulated by the non-receptor type protein tyrosine phosphatase 14. *Oncogene* **2013**;32(17):2220-9.

20. Lee JE, Park HS, Lee D, Yoo G, Kim T, Jeon H, et al. Hippo pathway effector YAP

inhibition restores the sensitivity of EGFR-TKI in lung adenocarcinoma having primary or acquired EGFR-TKI resistance. *Biochem Biophys Res Commun* **2016**;474:154−60.

21. Lee TF, Tseng YC, Chang WC, Chen YC, Kao YR, Chou TY, et al. YAP1 is essential for tumor growth and is a potential therapeutic target for EGFR-dependent lung adenocarcinomas. *Oncotarget* **2017**;8:89539−51.

22. Song S, Xie M, Scott AW, Jin J, Ma L, Dong X, et al. A Novel YAP1 Inhibitor Targets CSC-Enriched Radiation-Resistant Cells and Exerts Strong Antitumor Activity in Esophageal Adenocarcinoma. *Mol Cancer Ther* **2018**;17:443−54.

23. Kaneda A, Seike T, Danjo T, Nakajima T, Otsubo N, Yamaguchi D, et al. The novel potent TEAD inhibitor, K-975, inhibits YAP1/TAZ-TEAD protein-protein interactions and exerts an anti-tumor effect on malignant pleural mesothelioma. *Am J Cancer Res* **2020**;10:4399−415.

24. Kurppa KJ, Liu Y, To C, Zhang T, Fan M, Vajdi A, et al. Treatment-Induced Tumor Dormancy through YAP-Mediated Transcriptional Reprogramming of the Apoptotic Pathway. *Cancer Cell* **2020**;37(1):104-22.

25. Tang TT, Konradi AW, Feng Y, Peng X, Ma M, Li J, et al. Small Molecule Inhibitors of TEAD Auto-palmitoylation Selectively Inhibit Proliferation and Tumor Growth of NF2-deficient Mesothelioma. *Mol Cancer Ther* **2021**;20:986−98.

26. Lin KC, Park HW, Guan KL. Regulation of the Hippo Pathway Transcription Factor TEAD. *Trends Biochem Sci* **2017**;42:862−72.

27. Li Q, Sun Y, Jarugumilli GK, Liu S, Dang K, Cotton JL, et al. Lats1/2 Sustain Intestinal Stem Cells and Wnt Activation through TEAD-Dependent and Independent Transcription. *Cell Stem Cell* **2020**;26:675−92.e8.

28. Yap TA, Kwiatkowski DJ, Desai J, Dagogo-Jack I, Millward M, Kindler HL, et al. First-in-class, first-in-human phase 1 trial of VT3989, an inhibitor of yes-associated protein (YAP)/transcriptional enhancer activator domain (TEAD), in patients (pts) with advanced solid tumors enriched for malignant mesothelioma and other tumors with neurofibromatosis 2 (NF2) mutations. Presented at American Association for Cancer Research Annual Meeting 2023, Orlando, FL. 16 April 2023, in Proceedings of the American Association for Cancer Research Annual Meeting 2023, *Cancer Res.* **2023**;83(8_Supplement):Abstract nr CT006.

29. Tsuji T, Ozasa H, Aoki W, Aburaya S, Funazo T, Furugaki K, et al. Alectinib Resistance in ALK-Rearranged Lung Cancer by Dual Salvage Signaling in a Clinically Paired Resistance Model. *Mol Cancer Res* **2019**;17:212−24.

30. Crystal AS, Shaw AT, Sequist LV, Friboulet L, Niederst MJ, Lockerman EL, et al. Patient-derived models of acquired resistance can identify effective drug combinations

for cancer. *Science* **2014**;346(6216):1480-6.

31. Ozasa H, Oguri T, Maeno K, Takakuwa O, Kunii E, Yagi Y, et al. Significance of c-MET overexpression in cytotoxic anticancer drug-resistant small-cell lung cancer cells. *Cancer Sci* **2014**;105:1032−9.

32. Yasuda Y, Ozasa H, Kim YH, Yamazoe M, Ajimizu H, Yamamoto Funazo T, et al. MCL1 inhibition is effective against a subset of small-cell lung cancer with high MCL1 and low BCL-XL expression. *Cell Death Dis* **2020**;11:177.

33. Gallant JN, Sheehan JH, Shaver TM, Bailey M, Lipson D, Chandramohan R, et al. EGFR Kinase Domain Duplication (EGFR-KDD) Is a Novel Oncogenic Driver in Lung Cancer That Is Clinically Responsive to Afatinib. *Cancer Discov* **2015**;5:1155−63.

34. Du Z, Brown BP, Kim S, Ferguson D, Pavlick DC, Jayakumaran G, et al. Structure-function analysis of oncogenic EGFR Kinase Domain Duplication reveals insights into activation and a potential approach for therapeutic targeting. *Nat Commun* **2021**;12:1382.

35. Namba K, Shien K, Takahashi Y, Torigoe H, Sato H, Yoshioka T, et al. Activation of AXL as a Preclinical Acquired Resistance Mechanism Against Osimertinib Treatment in EGFR-Mutant Non-Small Cell Lung Cancer Cells. *Mol Cancer Res* **2019**;17(2):499-507.

36. Si J, Ma Y, Lv C, Hong Y, Tan H, Yang Y. HIF1A-AS2 induces osimertinib resistance in lung adenocarcinoma patients by regulating the miR-146b-5p/IL-6/STAT3 axis. *Mol*

Ther Nucleic Acids **2021**;26:613-24.

37. Sun Y, Meyers BA, Czako B, Leonard P, Mseeh F, Harris AL, et al. Allosteric SHP2 Inhibitor, IACS-13909, Overcomes EGFR-Dependent and EGFR-Independent Resistance Mechanisms toward Osimertinib. *Cancer Res* **2020**;80:4840−53.

38. Wang Y, Dong Q, Zhang Q, Li Z, Wang E, Qiu X. Overexpression of yes-associated protein contributes to progression and poor prognosis of non-small-cell lung cancer. *Cancer Sci* **2010**;101:1279−85.

39. Hong SA, Jang SH, Oh MH, Kim SJ, Kang JH, Hong SH. Overexpression of YAP1 in EGFR mutant lung adenocarcinoma prior to tyrosine kinase inhibitor therapy is associated with poor survival. *Pathol Res Pract* **2018**;214:335−42.

40. Zhao B, Ye X, Yu J, Li L, Li W, Li S, et al. TEAD mediates YAP-dependent gene induction and growth control. *Genes Dev.* **2008**;22:1962−71.

41. Coggins GE, Farrel A, Rathi KS, Hayes CM, Scolaro L, Rokita JL, et al. YAP1 Mediates Resistance to MEK1/2 Inhibition in Neuroblastomas with Hyperactivated RAS Signaling. *Cancer Res.* **2019**;79:6204−14.

42. Piccolo S, Dupont S, Cordenonsi M. The biology of YAP/TAZ: hippo signaling and beyond. *Physiol Rev* **2014**;94:1287−312.

Figure legends

Figure 1.

Patient-derived *EGFR* mutation-positive lung cancer cell line KTOR27.

A, Computed tomography image of the patient during afatinib treatment and a schematic explanation of the establishment of the patient-derived cell line. **B,** EGFR protein levels in PC-9, HCC827, and KTOR27 cells, as confirmed by immunoblotting. **C,** Cell viability assays of KTOR27 cells treated with afatinib, osimertinib, or alectinib for 72 h. **D,** KTOR27 cells were treated with the indicated concentrations of afatinib for 6 h. The cell lysates were analyzed by immunoblotting with the indicated antibodies. Results are expressed as the mean ± SEM. EGFR: epidermal growth factor receptor.

Figure 2.

YAP1 inhibition increased sensitivity to osimertinib treatment in KTOR27 cells *in vitro*.

A, Immunofluorescent staining of KTOR27 cells treated with afatinib (400 nmol/L) for 72 h. Cells were stained with the YAP1 antibody and Hoechst stain. White arrows indicate typical cells with YAP1 nuclear localization. **B,** Relative percentage of afatinib-treated KTOR27 cells with YAP1 nuclear localization. **C,** Relative gene expression of *YAP1* normalized to that of *GAPDH* after the siRNA knockdown of *YAP1* by two different

YAP1-directed RNAi sequences (si*YAP1*-A and si*YAP1*-B) in KTOR27 cells (left panel). Cell viability assays of KTOR27 cells transfected with *YAP1* siRNA or negative control siRNA and treated with afatinib for 72 h (right panel). **D,** Cell viability assays of KTOR27 cells treated with afatinib or osimertinib in the presence of VT104 for 7 days. **E,** Apoptosis assay using the caspase-Glo 3/7 Assay in KTOR27 cells exposed to afatinib and VT104 (500 nmol/L). **F,** Relative expression of *CTGF* normalized to that of *GAPDH* in KTOR27 cells treated with afatinib in the presence or absence of VT104 (500 nmol/L) for 72 h. Results are expressed as the mean ± SEM. $*p < 0.05$. YAP1: yes-associated protein 1. siRNA: small interfering RNA. RNAi: RNA interference. CTGF, connective tissue growth factor.

Figure 3.

YAP1 was activated by osimertinib treatment in PC-9 and HCC827 cells.

A, Relative cell viability in combination with library compounds and osimertinib in PC9 cells. **B,** Cell viability assays of PC-9 and HCC827 cells treated with osimertinib for 72 h. **C,** PC-9 and HCC827 cells were treated with the indicated concentrations of osimertinib for 6 h. The cell lysates were analyzed by immunoblotting with the indicated antibodies. **D and E,** Immunofluorescent staining of PC-9 and HCC827 cells treated with

osimertinib for 72 h. Cells were stained with the YAP1 antibody and Hoechst stain. **F,** Relative percentages of osimertinib-treated PC9 and HCC827 cells with YAP1 nuclear localization. Results are expressed as the mean ± SEM. *$p < 0.05$. n.s.: not significant. EGFR: epidermal growth factor receptor. YAP1: yes-associated protein 1.

Figure 4.

YAP1 inhibition increased sensitivity to osimertinib treatment in PC-9 and HCC827 cells *in vitro*.

A, Relative expression of *YAP1* normalized to that of *GAPDH* after siRNA knockdown of *YAP1* by two different *YAP1*-directed RNAi sequences (si*YAP1*-A and si*YAP1*-B) in PC-9 and HCC827 cells. **B,** Cell viability assays of PC-9 and HCC827 cells transfected with *YAP1* siRNA or negative control siRNA and treated with osimertinib for 72 h. **C,** Cell viability assays of PC-9 and HCC827 cells treated with osimertinib in the presence of VT104 for 7 days. **D,** Apoptosis assays using the caspase-Glo 3/7 Assay in PC9 and HCC827 cells treated with osimertinib and VT104. **E,** Relative expression of *CTGF* normalized to that of *GAPDH* in PC9 and HCC827 cells treated with osimertinib in the presence or absence of VT104 for 72 h. Results are expressed as the mean ± SEM. *$p < 0.05$. n.s.: not significant. YAP1: yes-associated protein 1. siRNA: small interfering

RNA. CTGF: connective tissue growth factor.

Figure 5.

Combination therapy of VT104 and osimertinib considerably suppressed tumor regrowth compared to osimertinib monotherapy in *EGFR* mutation-positive lung cancer cells *in vivo*.

A, Xenograft models were treated with vehicle, VT104 monotherapy (10 mg/kg, orally, daily), osimertinib monotherapy (5 mg/kg, orally, daily), or a combination of osimertinib and VT104 for 14 days. **B and C,** Tumor volume curves after vehicle treatment, VT104 monotherapy, osimertinib monotherapy, and combination therapy with osimertinib and VT104 (left). Percent body weight change in xenograft mice bearing PC-9 or HCC827 cells during and after the indicated treatments (right). **D,** Tumor volume on the last day of osimertinib monotherapy and combination therapy with osimertinib and VT104. Results are expressed as the mean ± SEM. $*p < 0.05$. EGFR: Epidermal growth factor receptor.

Figure 6.

Association between the clinical outcomes and immunohistochemical YAP1 expression

in TMA of *EGFR* mutation-positive lung cancers

A, Immunohistochemical YAP1 expression with nuclear localization or cytoplasmic localization in TMA of *EGFR* mutation-positive lung cancers. **B,** Kaplan–Meier curves of progression-free survival after EGFR-TKI administration according to the YAP1 localization status. **C,** Schematics of the initial survival mechanisms of EGFR-TKIs in *EGFR* mutation-positive lung cancer. YAP1: yes-associated protein 1. TMA: tissue microarray. EGFR: epidermal growth factor receptor. TKI: tyrosine kinase inhibitor. CI: confidence interval.

Figure 1

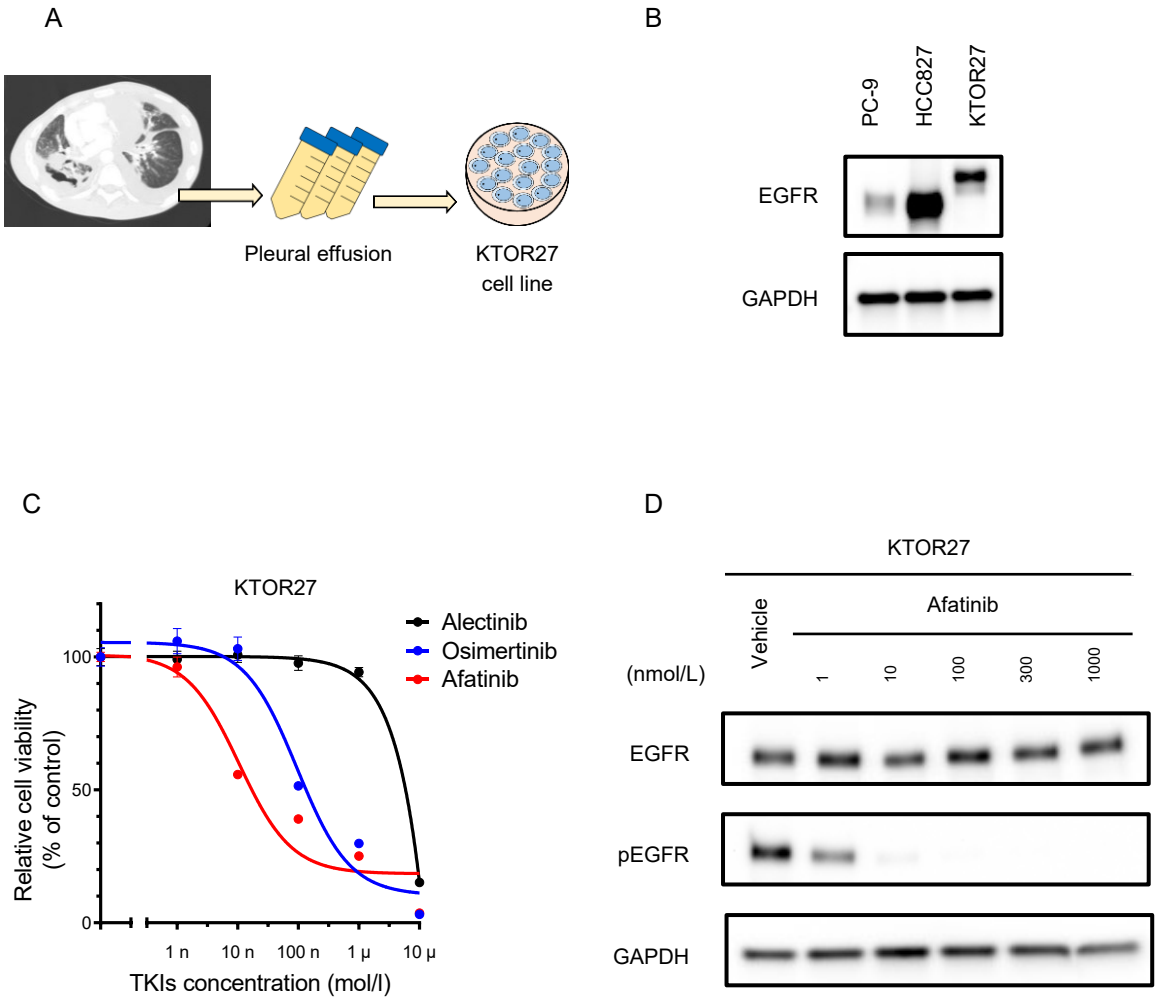
A
Pleural effusion
KTOR27
cell line
B
PC-9
HCC827
KTOR27
EGFR
GAPDH
C
KTOR27
Alectinib
Osimertinib
Afatinib
Relative cell viability
(% of control)
100
50
0
1 n
10 n
100 n
1 μ
10 μ
TKIs concentration (mol/l)
D
KTOR27
Vehicle
Afatinib
(nmol/L)
1
10
100
300
1000
EGFR
pEGFR
GAPDH

Figure 2

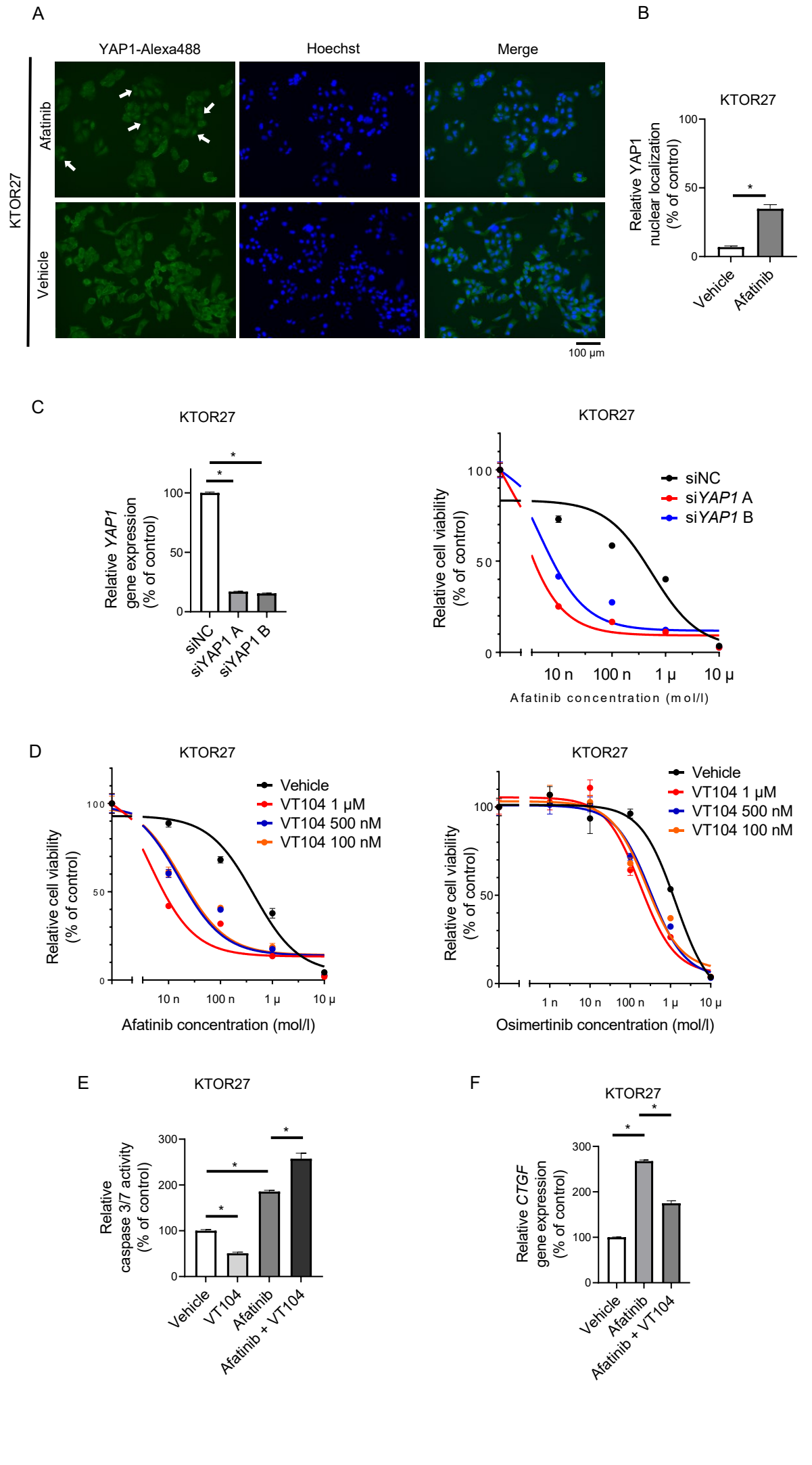
A
YAP1-Alexa488
Hoechst
Merge
KTOR27
Afatinib
Vehicle
100 μm
B
KTOR27
Relative YAP1 nuclear localization (% of control)
100
50
0
*
Vehicle
Afatinib
C
KTOR27
Relative YAP1 gene expression (% of control)
100
50
0
*
*
siNC
siYAP1 A
siYAP1 B
KTOR27
Relative cell viability (% of control)
100
50
0
siNC
siYAP1 A
siYAP1 B
10 n
100 n
1 μ
10 μ
Afatinib concentration (mol/l)
D
KTOR27
Relative cell viability (% of control)
100
50
0
Vehicle
VT104 1 μM
VT104 500 nM
VT104 100 nM
10 n
100 n
1 μ
10 μ
Afatinib concentration (mol/l)
KTOR27
Relative cell viability (% of control)
100
50
0
Vehicle
VT104 1 μM
VT104 500 nM
VT104 100 nM
1 n
10 n
100 n
1 μ
10 μ
Osimertinib concentration (mol/l)
E
KTOR27
Relative caspase 3/7 activity (% of control)
300
200
100
0
*
*
*
Vehicle
VT104
Afatinib
Afatinib + VT104
F
KTOR27
Relative CTGF gene expression (% of control)
300
200
100
0
*
*
Vehicle
Afatinib
Afatinib + VT104

Figure 3

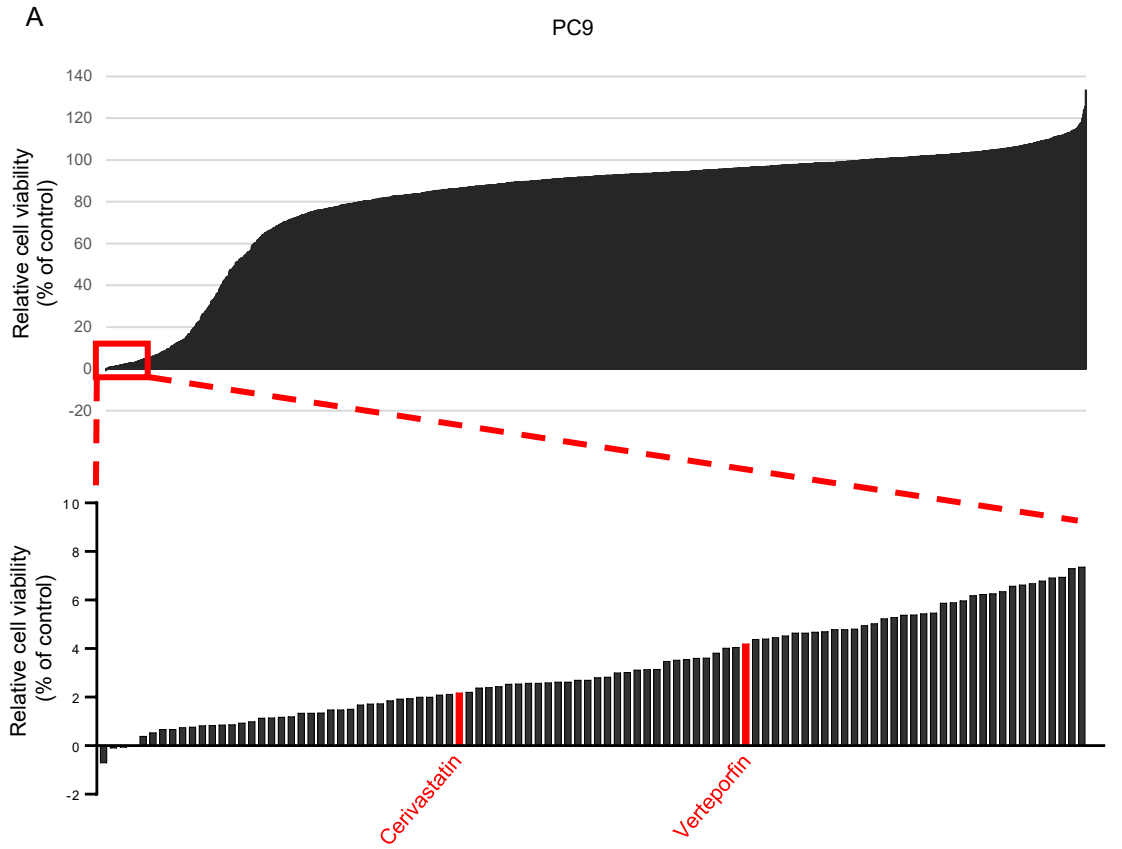

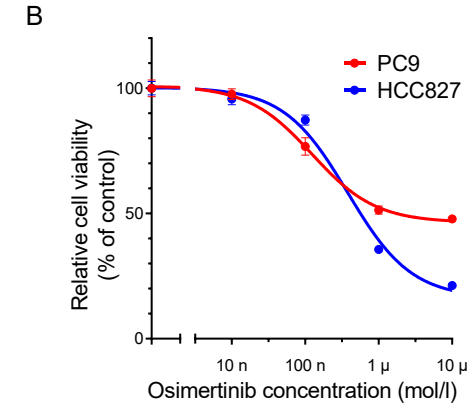

		IC_{50} (nmol/L)
PC9	Osimertinib	123
HCC827	Osimertinib	379

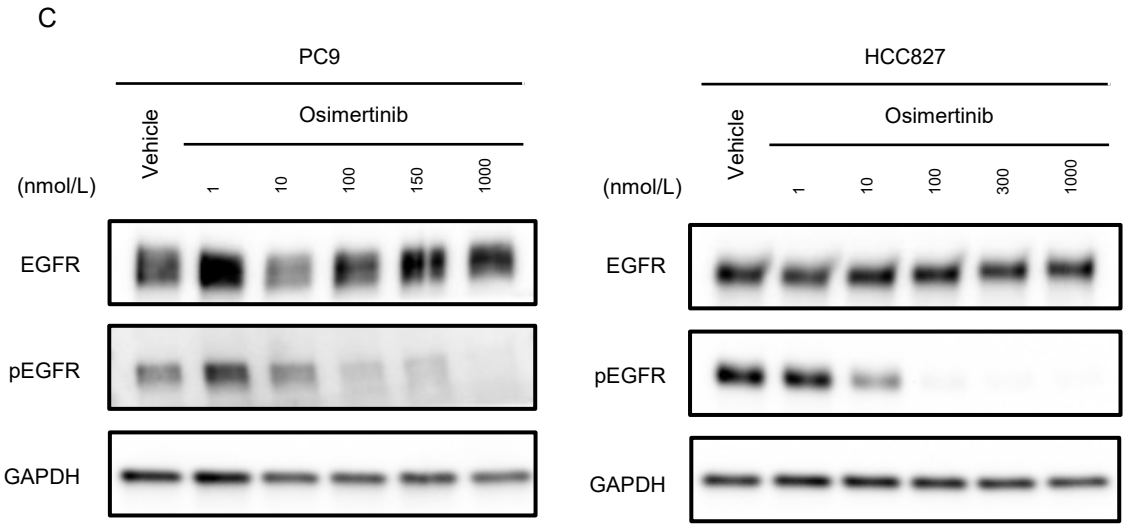

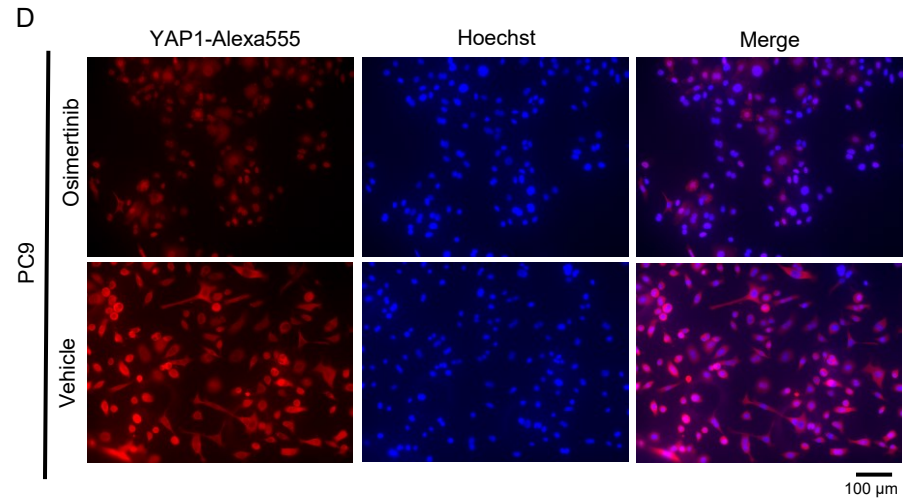
D
YAP1-Alexa555
Hoechst
Merge
PC9
Osimertinib
Vehicle
100 μm

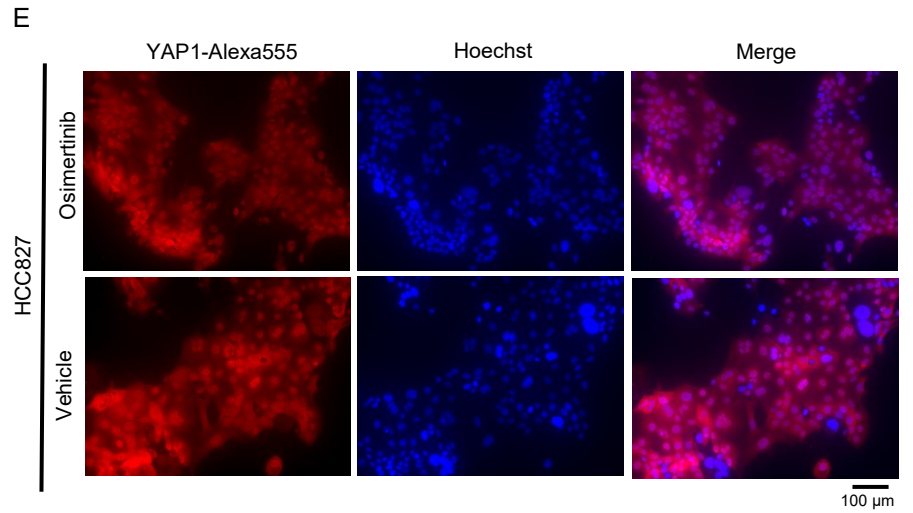
E
YAP1-Alexa555
Hoechst
Merge
HCC827
Osimertinib
Vehicle
100 μm

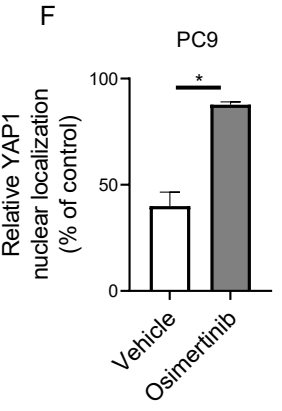
F
PC9
Relative YAP1 nuclear localization (% of control)
100
50
0
*
Vehicle
Osimertinib

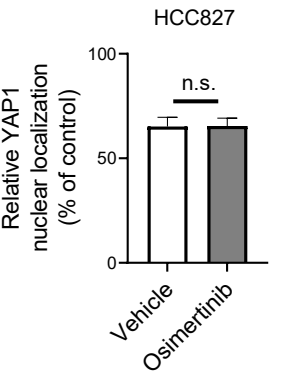
HCC827
Relative YAP1 nuclear localization (% of control)
100
50
0
n.s.
Vehicle
Osimertinib

Figure 4

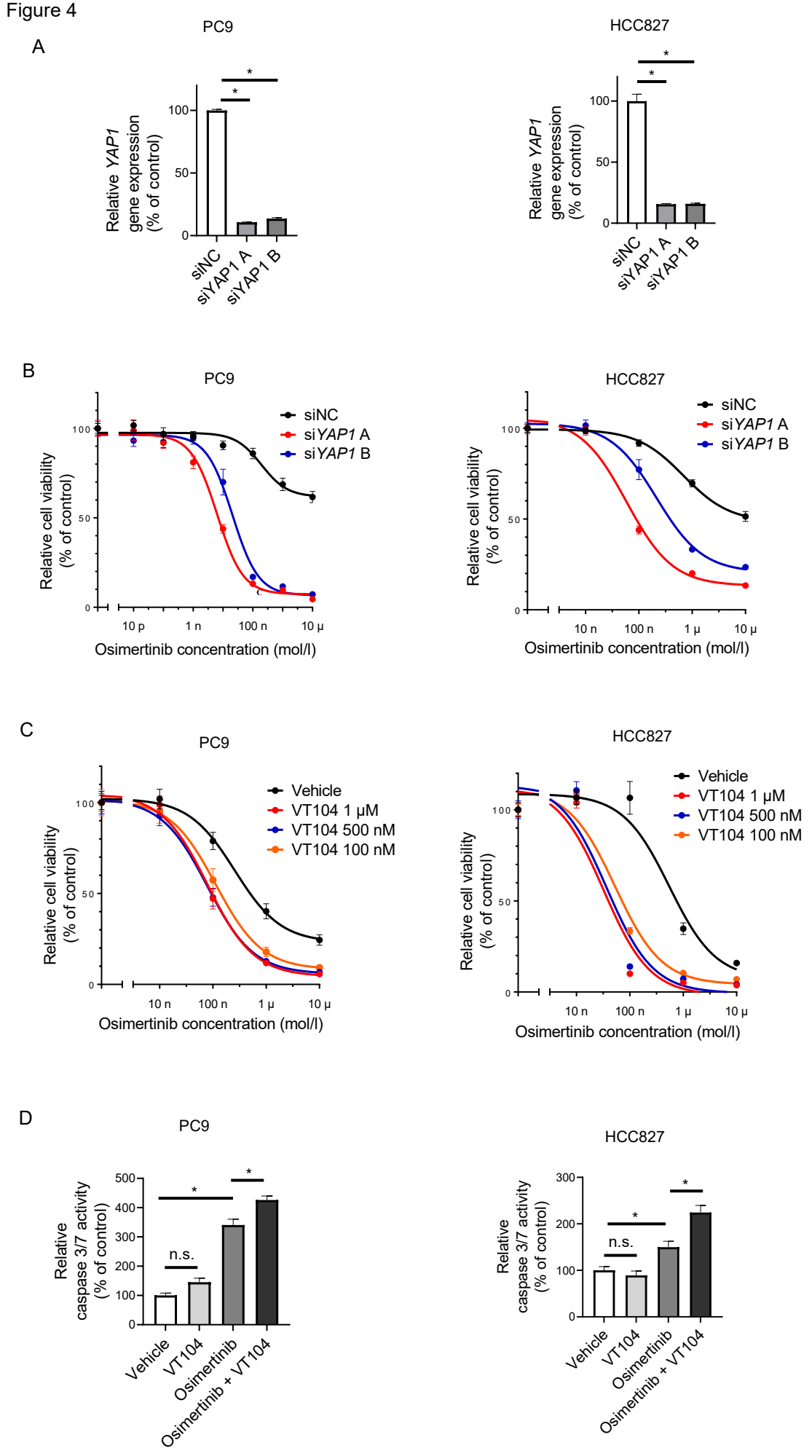
A
PC9
HCC827
Relative YAP1 gene expression (% of control)
siNC
siYAP1 A
siYAP1 B
B
Relative cell viability (% of control)
Osimertinib concentration (mol/l)
C
Vehicle
VT104 1 μM
VT104 500 nM
VT104 100 nM
D
Relative caspase 3/7 activity (% of control)
n.s.
Vehicle
VT104
Osimertinib
Osimertinib + VT104

E

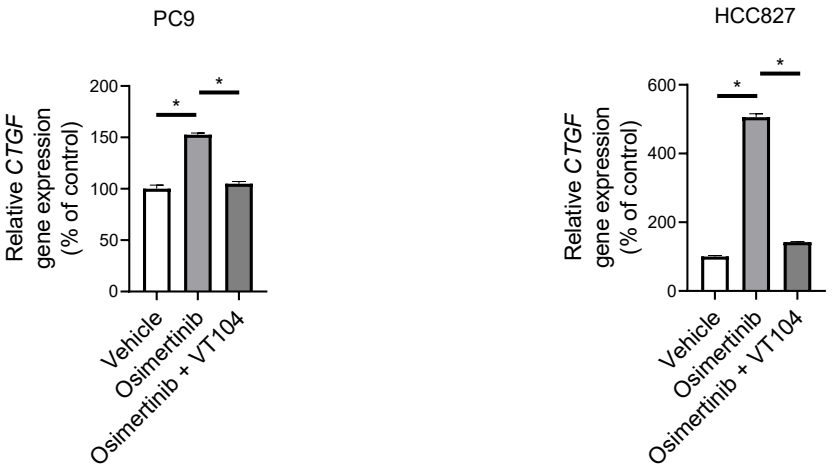
PC9
HCC827
Relative CTGF gene expression (% of control)
200
150
100
50
0
600
400
200
0
*
*
*
*
Vehicle
Osimertinib
Osimertinib + VT104

Figure 5

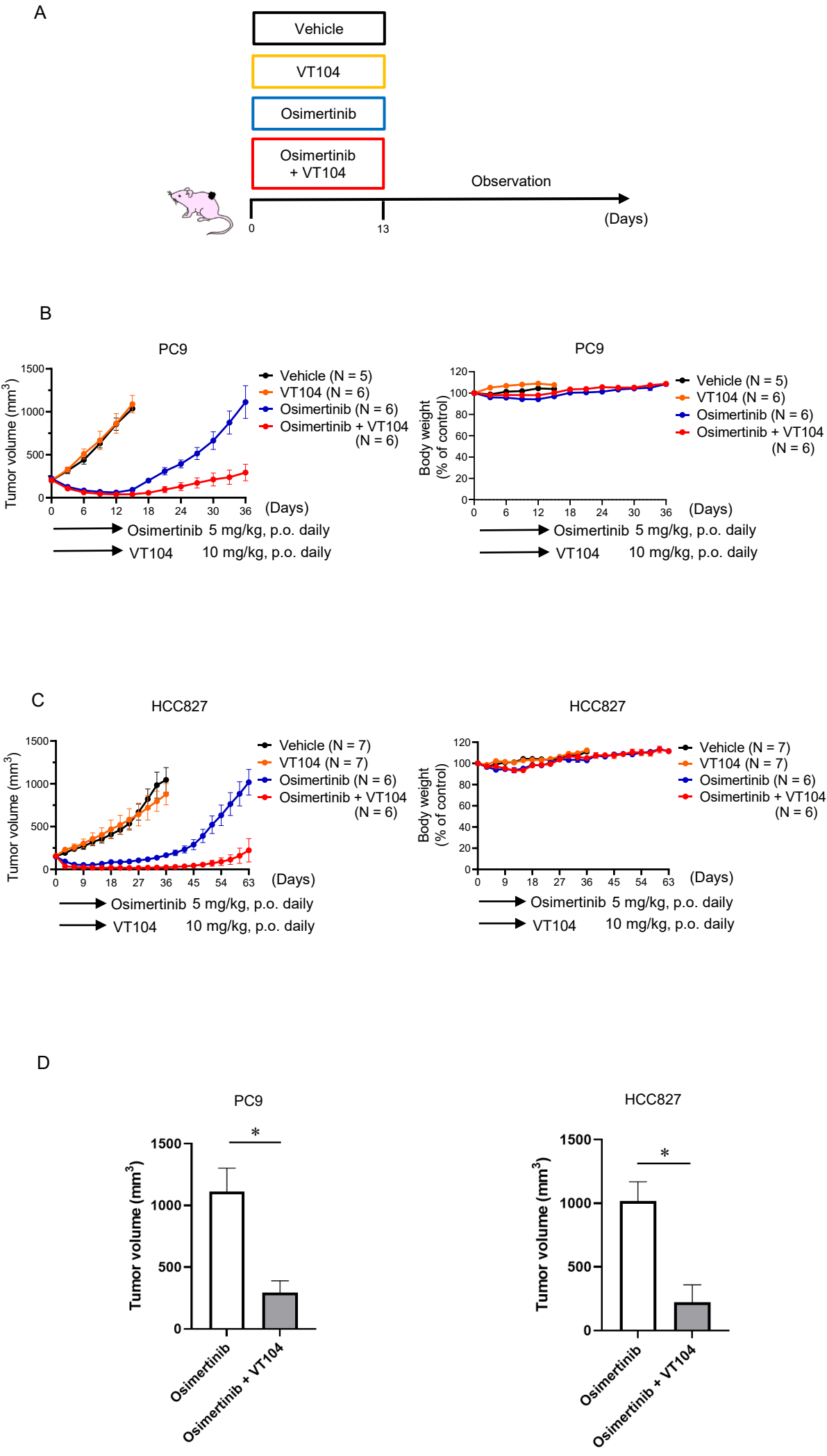
A
Vehicle
VT104
Osimertinib
Osimertinib + VT104
Observation
0
13
(Days)
B
PC9
Tumor volume (mm3)
Vehicle (N = 5)
VT104 (N = 6)
Osimertinib (N = 6)
Osimertinib + VT104 (N = 6)
(Days)
Osimertinib 5 mg/kg, p.o. daily
VT104 10 mg/kg, p.o. daily
PC9
Body weight (% of control)
Vehicle (N = 5)
VT104 (N = 6)
Osimertinib (N = 6)
Osimertinib + VT104 (N = 6)
(Days)
Osimertinib 5 mg/kg, p.o. daily
VT104 10 mg/kg, p.o. daily
C
HCC827
Tumor volume (mm3)
Vehicle (N = 7)
VT104 (N = 7)
Osimertinib (N = 6)
Osimertinib + VT104 (N = 6)
(Days)
Osimertinib 5 mg/kg, p.o. daily
VT104 10 mg/kg, p.o. daily
HCC827
Body weight (% of control)
Vehicle (N = 7)
VT104 (N = 7)
Osimertinib (N = 6)
Osimertinib + VT104 (N = 6)
(Days)
Osimertinib 5 mg/kg, p.o. daily
VT104 10 mg/kg, p.o. daily
D
PC9
Tumor volume (mm3)
*
Osimertinib
Osimertinib + VT104
HCC827
Tumor volume (mm3)
*
Osimertinib
Osimertinib + VT104

Figure 6

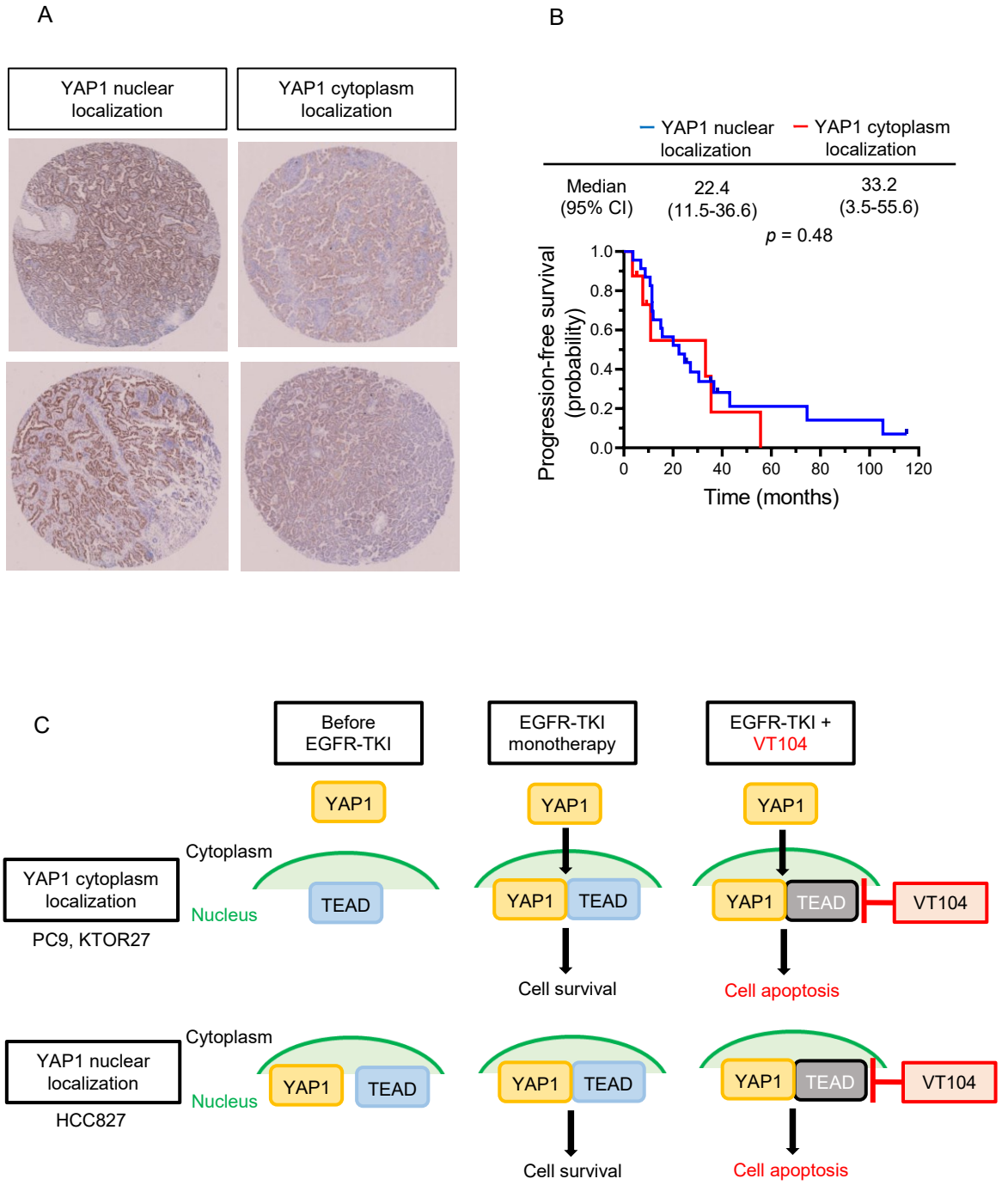
A
YAP1 nuclear localization
YAP1 cytoplasm localization
B
YAP1 nuclear localization
YAP1 cytoplasm localization
Median (95% CI)
22.4 (11.5-36.6)
33.2 (3.5-55.6)
p = 0.48
Progression-free survival (probability)
1.0
0.8
0.6
0.4
0.2
0.0
0
20
40
60
80
100
120
Time (months)
C
Before EGFR-TKI
EGFR-TKI monotherapy
EGFR-TKI + VT104
YAP1
TEAD
VT104
Cytoplasm
Nucleus
YAP1 cytoplasm localization
PC9, KTOR27
YAP1 nuclear localization
HCC827
Cell survival
Cell apoptosis